J. Phys.: Condens. Matter **12** (2000) 2867–2875. Printed in the UK PII: S0953-8984(00)10039-6

# Far-infrared study of the insulator–metal transition in $\kappa$-(BEDT-TTF)$_2$Cu(NCS)$_2$: evidence for polaron absorption

N L Wang†‡, B P Clayman‡, H Mori§ and S Tanaka§

† Institute of Physics and Centre for Condensed Matter Physics, Chinese Academy of Sciences, PO Box 2711, Beijing 100080, People's Republic of China
‡ Department of Physics, Simon Fraser University, Burnaby, British Columbia, Canada, V5A 1S6
§ Superconductivity Research Laboratory, ISTEC, Shinonome 1-10-13, Tokyo 135-0062, Japan

Received 2 December 1999, in final form 3 February 2000

**Abstract.** We present the infrared properties of $\kappa$-(BEDT-TTF)$_2$Cu(NCS)$_2$ for $\boldsymbol{E} \parallel \boldsymbol{b}$ and $\boldsymbol{E} \parallel \boldsymbol{c}$ focusing on the evolution of charge conduction from high-$T$ insulating to low-$T$ metallic behaviour. Anomalous absorption manifested in a broad peak in the optical conductivity at high temperature is interpreted in terms of photon-assisted hopping of small polarons. A sharp Drude peak that develops at low temperature, together with large mid-infrared spectral weight in the conductivity, are attributed to coherent and incoherent bands of large polarons. The insulator–metal transition can be understood as a crossover from localized small-polaron to coherent large-polaron behaviour.

Among various organic compounds containing electron–donor BEDT-TTF (abbreviated as ET) molecules, the $\kappa$-phase family $\kappa$-(ET)$_2$X, where X is an anion, has attracted much attention because they show a variety of electronic phases including antiferromagnetic (AF) insulator, paramagnetic insulator, paramagnetic metal, and superconductor. They have a two-dimensional (2D) layer structure consisting of conducting ET sheets and insulating anion X sheets (in the $bc$-plane). The temperature–pressure phase diagram of $\kappa$-(ET)$_2$X resembles that of strongly correlated systems such as $V_2O_3$ and $NiS_{2-x}Se_x$ [1]. $\kappa$-(ET)$_2$Cu[N(CS)$_2$]Cl is an antiferromagnetic insulator at ambient pressure [2]. With increasing pressure, this salt undergoes a superconducting transition at 13 K at 0.3 kbar, above which temperature a broad peak is seen in the resistivity curve which separates regions of low-$T$ metallic and high-$T$ insulating transport [3]. This kind of unusual $T$-dependent resistivity has been found in $\kappa$-(ET)$_2$Cu(NCS)$_2$ at ambient pressure above its superconducting transition temperature 10.4 K [4]. The resistivity peak appears at around 90 K. Further pressure leads to suppression of both the superconductivity and the resistivity maximum.

The AF insulating phase has been described as a Hubbard–Mott insulator, considering the dimerization of ET molecules which effectively makes the system have one hole per dimer [5]. Although no AF long-range ordering has been found for $\kappa$-(ET)$_2$Cu(NCS)$_2$, strong AF spin fluctuations exist in this material at ambient pressure [6]. The peculiarity in the dc resistivity is in fact the manifestation of the anomalous properties of the material near the Mott transition. Therefore, it is of great interest to clarify the nature of the charge dynamics, in particular the origin of the broad peak in the $T$-dependent resistivity. Several different mechanisms have been proposed to explain this unusual transport, including localization [4], band-gap opening [7], and polaron formation [8]. However, no consensus has been reached.

0953-8984/00/122867+09$30.00  

Optical spectroscopy is an important technique for probing the electronic state of a material. Though there were several previous reports of reflectivity results [9–12], little attention was given to the origin of the temperature-controlled insulator–metal transition. In this study, we report the detailed temperature dependence of the infrared properties of $\kappa$-$(ET)_2Cu(NCS)_2$ with $\boldsymbol{E} \parallel \boldsymbol{b}$ and $\boldsymbol{E} \parallel \boldsymbol{c}$, in an attempt to understand the charge dynamics across the transition from high-$T$ insulating to low-$T$ metallic transport. Our results provide strong evidence for polaron absorption. In particular, the spectra reveal a crossover from a small-polaron-dominated regime at high $T$ to a large-polaron-dominated regime at low $T$.

Salts of $\kappa$-$(ET)_2Cu(NCS)_2$ were prepared by an electrochemical method [4]. Optical reflectivity spectra were measured from 50 $cm^{-1}$ to 9500 $cm^{-1}$ on a Bruker 113v spectrometer using an *in situ* overcoating technique [13]. The optical conductivity was calculated via a Kramers–Kronig analysis of the reflectivity. For this analysis, $R(\omega)$ below 50 $cm^{-1}$ was extrapolated with the Hagen–Rubens relation. The conductivity in the measured frequency range is found to be insensitive to different extrapolations at low $\omega$. For the high-frequency region, we extrapolated the measured spectrum at 9500 $cm^{-1}$ as constant to 160 000 $cm^{-1}$, above which a $\omega^{-4}$-relation was employed.

The measured reflectivities at various temperatures in polarizations $\boldsymbol{E} \parallel \boldsymbol{b}$ and $\boldsymbol{E} \parallel \boldsymbol{c}$ are shown in figures 1(a) and 1(b), respectively. The spectra evolve with temperature in a similar way for both polarizations. For $T > 80$ K, reflectivity is low in the far-infrared (FIR) region, indicating non-metallic behaviour. This is qualitatively consistent with dc measurements. The reflectivity between 400 $cm^{-1}$ and 2000 $cm^{-1}$ increases monotonically as temperature decreases from room temperature. Below 80 K, the reflectivity in the FIR region increases sharply with temperature, reflecting an evolution towards metallic conduction.

The calculated real parts of conductivity at several temperatures for $\boldsymbol{E} \parallel \boldsymbol{b}$ and $\boldsymbol{E} \parallel \boldsymbol{c}$ are shown in figures 1(c) and 1(d). At high temperatures (for example, at 200 K), the electronic spectrum exhibits a broad peak at around 3700 $cm^{-1}$ for $\boldsymbol{E} \parallel \boldsymbol{b}$ and 2300 $cm^{-1}$ for $\boldsymbol{E} \parallel \boldsymbol{c}$. There is no Drude response at low frequency for either polarization, suggesting highly incoherent charge carriers. Though the conductivity below the frequency of the broad peak decreases with decreasing frequency, no evidence of an energy gap is observed. This indicates that the non-metallic conduction at high $T$ is not due to a typical gap opening in the charge excitation. As temperature decreases from room temperature to 80 K, the intensity of the broad peak increases. In addition, spectral weight below the peak frequency increases. But there remains no free-carrier contribution to the low-$\omega$ conductivity. With further decrease in temperature ($T < 80$ K), the broad peaks start decrease in intensity and free-carrier components develop rapidly. At around 10 K, sharp and narrow Drude components are observed in both polarizations.

There are two possibilities for the origin of the broad peak in the mid-infrared (MIR) region. One is an interband transition [12]. However, this scenario has difficulty in explaining the large amount of spectral weight at low frequency. Ignoring the response of phonons, we can see that the conductivity at high $T$ increases from almost zero frequency all the way up to its peak value for both polarizations (see, for example, the room-$T$ data in figure 2). The frequency range is too broad for this to be due to an interband transition. A more reasonable possibility is that the broad MIR peak is due to localized small-polaron absorption. Polaron formation due to the strong electron–phonon coupling has been proposed to explain unusual dc transport properties of this material [8], but has not been considered with respect to the electronic spectrum in optical conductivity.

According to theoretical investigations of small-polaron response [14], the optical conductivity should have low spectral weight in the FIR region, but a peak in the high-$\omega$ region. The low dc or FIR conductivity is associated with the activated hopping of self-

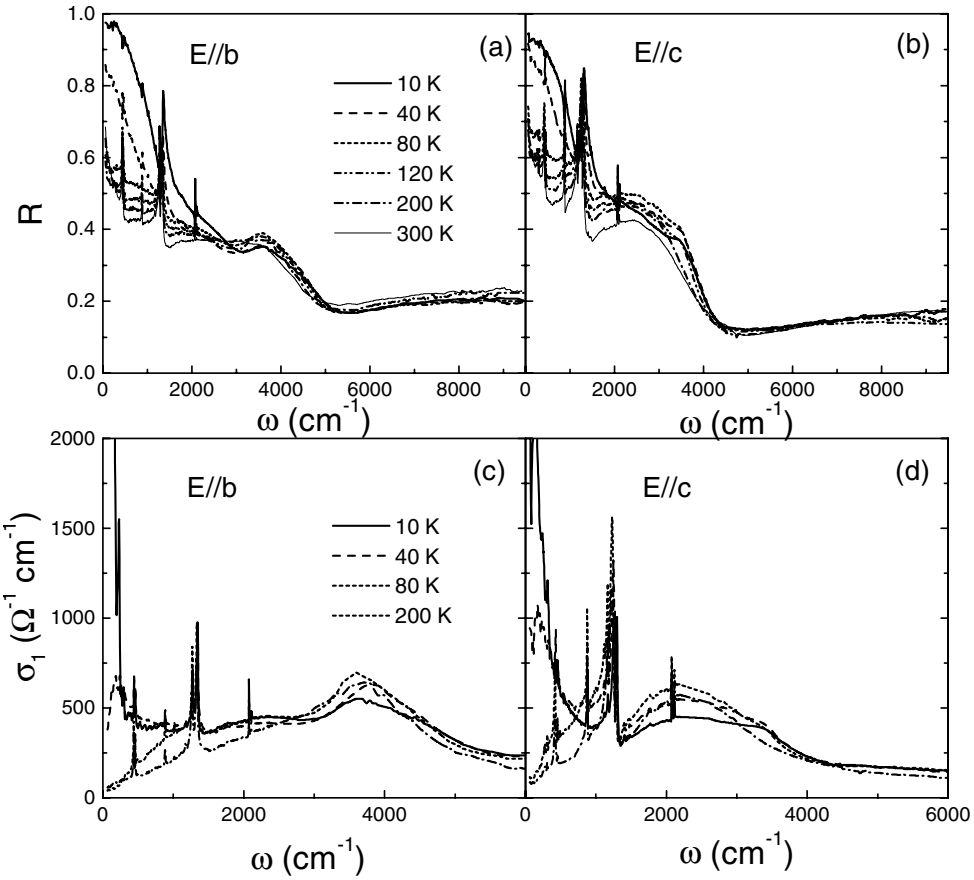


**Figure 1.** The frequency dependence of reflectivity and conductivity for $\boldsymbol{E} \parallel \boldsymbol{b}$ and $\boldsymbol{E} \parallel \boldsymbol{c}$ at several temperatures.

trapped carriers between localized sites, while the peak at high $\omega$ is due to the photon-assisted hopping (photoionization) of small polarons. Apparently, our conductivity spectra at high $T$ have those features. In particular, the increase of the strength of the MIR peak with decreasing temperature from 300 K to 80 K is consistent with the expected response of small polarons.

Quantitatively, the optical conductivity for a small polaron caused by strong electron–phonon interaction can be expressed as [14]

$$\sigma_{sp}(\omega, T) = \sigma(0, T)\exp[-(\hbar\omega)^2/\Delta^2]\frac{\sinh(4E_b\hbar\omega/\Delta^2)}{4E_b\hbar\omega/\Delta^2} \tag{1}$$

where $\sigma(0, T)$ is the dc conductivity, $E_b$ is the small-polaron binding energy, $\Delta = (8E_bE_{vib})^{1/2}$ is a broadening factor, and $E_{vib}$ is the characteristic vibration energy, which equals $k_BT$ at high temperatures. For sufficiently strong electron–lattice coupling, $E_b > E_{vib}$, the peak appears at $\hbar\omega \approx 2E_b$. Equation (1) has been used to quantify the effects of small polarons in $La_{1-x}Sr_xMnO_3$ [15], $La_{2-x}Sr_xNiO_4$ [16], $LaCoO_3$ [17], and $TiO_2$ [18]. In figures 2(a) and 2(b), we display the room temperature conductivities for $\boldsymbol{E} \parallel \boldsymbol{b}$ and $\boldsymbol{E} \parallel \boldsymbol{c}$ together with a fit using the above equation. We can see that the small-polaron picture provides a reasonable fit to the room-$T$ optical conductivity. The values of $E_b$ resulting from the analysis are 1940 cm$^{-1}$ (0.24 eV) for $\boldsymbol{E} \parallel \boldsymbol{b}$ and 1420 cm$^{-1}$ (0.18 eV) for $\boldsymbol{E} \parallel \boldsymbol{c}$, which are smaller than the values for

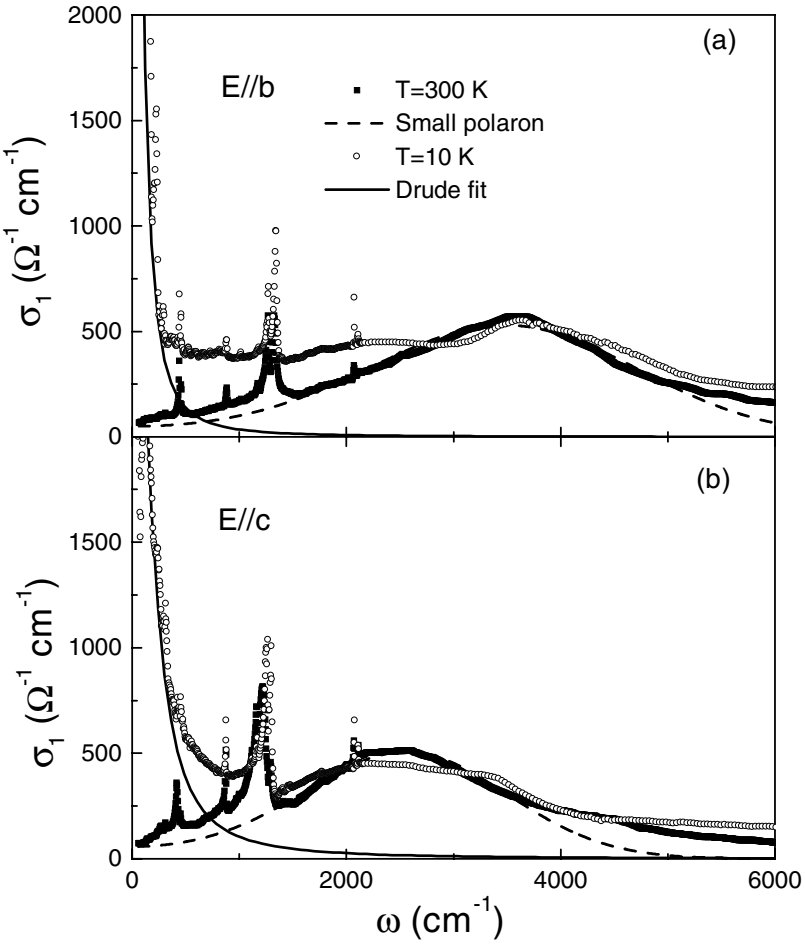


**Figure 2.** The frequency dependence of the conductivity for $\boldsymbol{E} \parallel \boldsymbol{b}$ (a) and $\boldsymbol{E} \parallel \boldsymbol{c}$ (b) at 300 K and 10 K. The solid curves are the Drude fits for the low-frequency free-carrier components. The dashed curves are calculated according to equation (1).

the above-mentioned small-polaron materials (about 0.24–0.29 eV for $La_{2-x}Sr_xNiO_4$, 0.35 eV for $LaCoO_3$, and 0.4 eV for $TiO_2$) [16–18]. Since small-polaron size is inversely proportional to the binding energy $E_b$, the larger value for $E_b$ with $\boldsymbol{E} \parallel \boldsymbol{b}$ may suggest a smaller polaron size in the *b*-direction than in the *c*-direction, or in other words, an anisotropic distortion.

In the literature, the small-polaron binding energies for some organic molecules were inferred by reference to determinations of the linear coupling constants of the intramolecular electron–phonon interaction, usually referred to as the electron–molecular-vibration (EMV) interaction [19–22]. Considering the influence of molecular symmetry on the selection rules, only totally symmetric (abbreviated by $a_g$) normal modes contribute to the small-polaron binding energy [19–22]. Using a semi-empirical MNDO method for the calculation of radical cation electronic structure and EMV coupling constants, Kozlov *et al* obtained a value of $E_b = 127$ meV for ET-derivative molecules [21]. A recent calculation by Visentini *et al* in terms of an isolated-dimer model yielded $E_b$ as only 68 meV [23]. The values that we get from the electronic spectra thus are somewhat larger than those based on the calculations of

EMV coupling constants of vibrational modes. It was previously realized that the value of $E_b$ extracted from the determination of the coupling constants is smaller than the observation from the photoemission measurement (0.29 eV for ET) [22, 24]. It was suggested that the discrepancy partly comes from neglect of quadratic EMV coupling in the calculation [22]. Theoretical work by Munn and Siebrand showed that quadratic coupling changes the energy of a polaron, and reduces its mobility very effectively [25]. Therefore, it has the same effect as an increase in binding energy for a polaron with linear coupling.

Our above analysis indicates that the electronic response of this ET salt at high temperature can be well understood in terms of a small-polaron absorption. Since polaron formation originates from strong electron–phonon coupling, information about the formation should be reflected in the vibrational spectrum. It should be pointed out that, although the small-polaron binding energy was determined for some organic salts on the basis of the evaluation of coupling constants of vibrational modes as we discussed above, it was only taken as a relative measure of the total EMV coupling strength [19–22], and there was no explicit discussion on the formation of polarons in those works. For this reason, we analyse the vibrational spectrum and try to deduce underlying polaron information.

Plotted in figures 3(a) and 3(b) are the strongest intramolecular vibrations at different temperatures for the two polarizations. The peaks at around 1330 cm$^{-1}$ for $\boldsymbol{E} \parallel \boldsymbol{b}$ and 1220 cm$^{-1}$ for $\boldsymbol{E} \parallel \boldsymbol{c}$ were assigned to the C=C stretching mode [10, 12]. Two notable features can be seen here. First, the peaks, superimposed on the electronic background, are asymmetrical (Fano shape). The low-$\omega$ side of the peak is elevated above its high-$\omega$ side. The asymmetrical phonon peak is an indication of strong electron–phonon coupling. Second, there is a significant shift of phonon frequency towards high $\omega$ (hardening) with decreasing temperature. To see this more clearly, we plot the frequency shift as a function of temperature for two normal modes for $\boldsymbol{E} \parallel \boldsymbol{b}$ and $\boldsymbol{E} \parallel \boldsymbol{c}$ in figures 4(a) and 4(b): the C=C stretching mode and the C–S stretching mode (at around 880 cm$^{-1}$) [10]. Interestingly, the frequency shifts are different for different modes. The C=C stretching mode exhibits the largest shift. Another prominent fact is that the hardening becomes much more pronounced after the material becomes metallic at around 80 K. Such a frequency shift is significantly different from a normal hardening with decreasing temperature. It provides further evidence of strong electron–phonon coupling.

Notably, the hardening of the normal modes is similar to that observed in the manganese oxides $La_{0.7}Sr_{0.3}MnO_3$ under the transition from high-$T$ paramagnetic insulating phase to low-$T$ ferromagnetic metallic phase [27]. Polaron formation in this material has been indicated by various experimental techniques; in particular, the unusual hardening of the phonon frequency associated with the insulator–metal transition was attributed to a crossover from a small- to a large-polaronic state due to an increase of polaron bandwidth with decreasing $T$ [27, 28]. We think that the phonon frequency shift in the present study can be understood via a similar picture. Of course, the origin of the bandwidth increase is different. In manganese oxides, the increase was caused by a double-exchange mechanism [28]. while in the present case it is due to other causes. A likely origin is the structure contraction which we shall discuss at the end of the paper.

Let us move on to the low-$T$ conductivity. After the material becomes metallic, the broad peak in the MIR region weakens; meanwhile a Drude-like response at low $\omega$ starts to develop. Let us concentrate on the conductivity spectra at the lowest temperature. In addition to a sharp Drude component at low frequency, the conductivity still has large spectral weight in the MIR region. This demonstrates that the metallic state of this material at low $T$ is rather unusual. By fitting the low-frequency peak to a Drude model (see figure 2), we estimate that the free-carrier contribution to the plasma frequency is 5400 cm$^{-1}$ for $\boldsymbol{E} \parallel \boldsymbol{b}$ and 6000 cm$^{-1}$ for $\boldsymbol{E} \parallel \boldsymbol{c}$. These

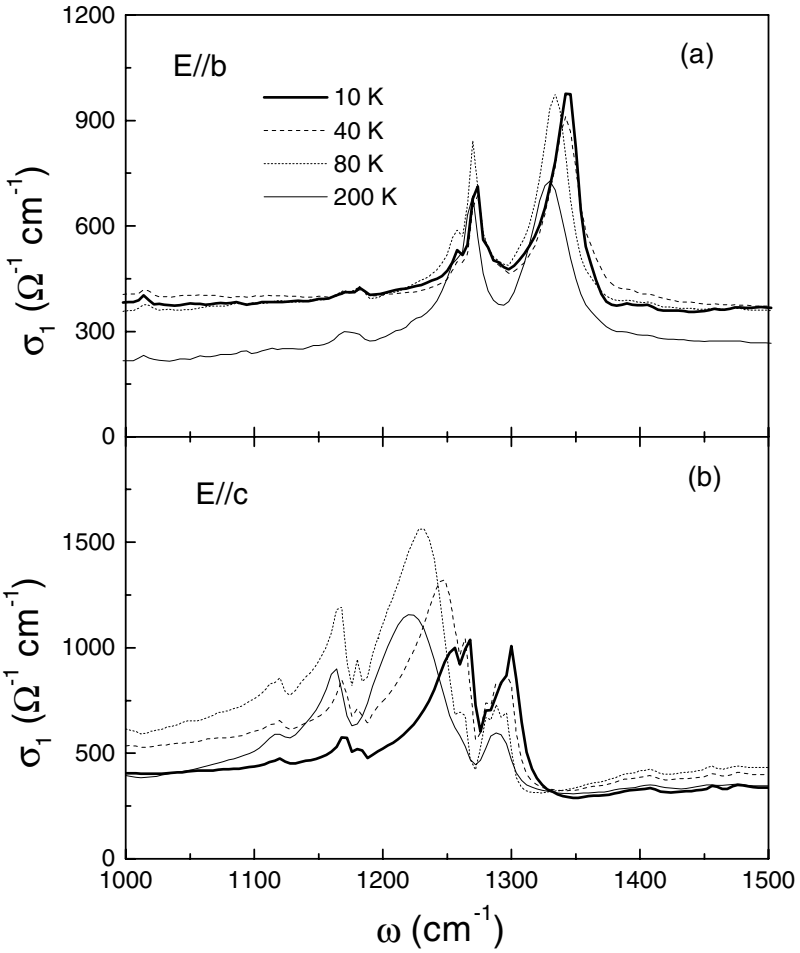


**Figure 3.** Expanded portions of the conductivity spectra for $\boldsymbol{E} \parallel \boldsymbol{b}$ (a) and $\boldsymbol{E} \parallel \boldsymbol{c}$ (b), showing features of major phonons at different temperatures.

values are close to earlier estimations directly from the reflectance spectra [9, 10]. We note that the Drude peak is narrower and sharper in the $b$-direction than in the $c$-direction, which correlates with a relatively higher dc conductivity in the $b$-direction.

The overall spectral weight obeys the sum rule

$$N_{eff}(\omega') = (2m^*V/\pi e^2)\int_0^{\omega'} \sigma(\omega)\,\mathrm{d}\omega \tag{2}$$

which is related to an equivalent overall plasma frequency by

$$\omega_p'^2 = 4\pi e^2 N_{eff}(\omega')/m^*V = 8\int_0^{\omega'} \sigma(\omega)\,\mathrm{d}\omega.$$

By integrating the conductivity to 6000 $\mathrm{cm}^{-1}$ where the spectrum shows a well-defined minimum, we get $\omega_p' = 10\,800\ \mathrm{cm}^{-1}$ for $\boldsymbol{E} \parallel \boldsymbol{b}$ and $10\,000\ \mathrm{cm}^{-1}$ for $\boldsymbol{E} \parallel \boldsymbol{c}$. The Drude contribution to the overall weight is small, about 1/4 for $\boldsymbol{E} \parallel \boldsymbol{b}$ and 1/3 for $\boldsymbol{E} \parallel \boldsymbol{c}$ at 10 K. The MIR component contains most of the low-energy spectral weight. This type of behaviour has

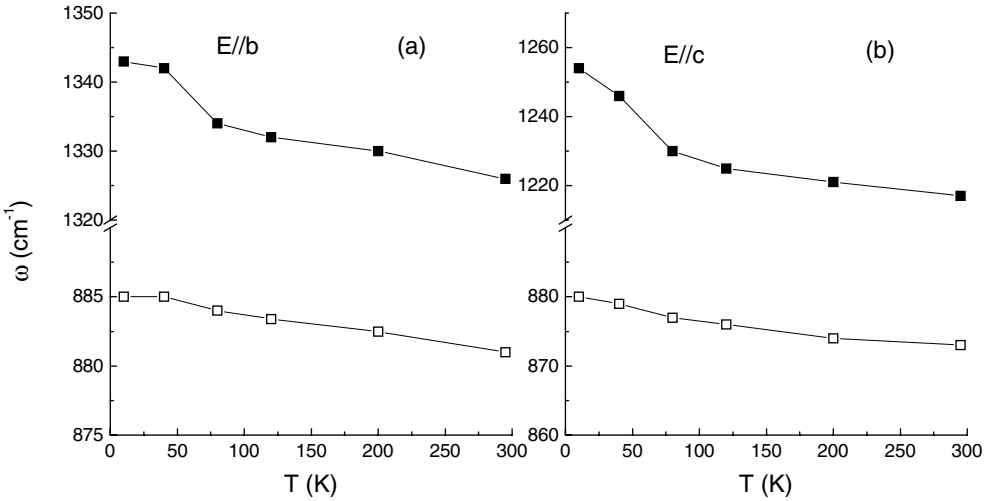


**Figure 4.** Phonon frequencies of the C=C stretching mode (solid squares) and the C–S stretching mode (empty squares) for $\boldsymbol{E} \parallel \boldsymbol{b}$ (a) and $\boldsymbol{E} \parallel \boldsymbol{c}$ (b) at various temperatures.

been observed in the double-exchange system $La_{1-x}Sr_xMnO_3$ in its ferromagnetic metallic state [29].

The most plausible explanation for the appearance of additional low-frequency conductivity at low $T$ remains polaron absorption. It is known that both coherent motion of large polarons and tunnelling of small polarons can result in metallic conduction. Though tunnelling conduction by small polarons at low $T$ has been proposed by Cariss *et al* from analysis of $T$-dependent dc resistivity of this material [8], we find that our results for the metallic response at low $T$ are better explained in terms of the large-polaron picture of Emin [14].

According to this theoretical picture of polaron absorption [14], a large polaron should contribute two parts to the optical conductivity: a free-carrier component at low $\omega$ and a broad incoherent band in the MIR region. The free-carrier component is due to the coherent motion of large polarons and should appear at frequencies below the characteristic phonon frequency and become more pronounced as $T$ decreases. The incoherent MIR band is due to the photoionization of large polarons; it is asymmetrical and has a long tail above its peak position. In contrast, the tunnelling of small polarons would produce a free-carrier absorption that is restricted to frequencies far below phonon frequencies. Both a sharp Drude peak at low $\omega$ and large spectral weight in the MIR seen in our spectra are quite consistent with polaron absorption characteristics. We note that the Drude components developed below 80 K are at frequencies roughly below the major phonon peaks; consequently, they are better attributed to the coherent motion of large polarons rather than to the tunnelling of small polarons†. The estimated Drude spectral weight, being about 1/3 of the overall spectral weight for $\boldsymbol{E} \parallel \boldsymbol{c}$ and 1/4 for $\boldsymbol{E} \parallel \boldsymbol{c}$, also suggests a large-polaron absorption, since, for small polarons, one should observe a much smaller Drude weight due to the restriction of the free-carrier component to very low frequencies.

The above analysis suggests a crossover from a small-polaron-dominated regime at high $T$ to a large-polaron-dominated regime at low $T$. The optical conductivity at high $T$ can be well explained by self-trapped small polarons and their photoionization, while the coherent

† In the $b$-direction, the Drude component appears in the lower-frequency region. Again, this may reflect the relatively smaller polaron size in this direction.

large polarons are responsible for the metallic dc transport and the Drude optical response at low $T$. The same conclusion was reached from the analysis of phonon frequency hardening. On the other hand, although the intensity of the MIR peaks decreases for both $\boldsymbol{E} \parallel \boldsymbol{b}$ and $\boldsymbol{E} \parallel \boldsymbol{c}$, they do not disappear completely. This indicates that coherent large polarons coexist with small polarons, which remain localized at low $T$.

Finally, we discuss what causes the crossover from a small- to a large-polaronic state. As stated earlier, such a crossover could result from an increase in polaron bandwidth, we would expect the bandwidth to increase with decreasing $T$. A possible origin for this bandwidth increase is the structure contraction. The lattice parameters versus $T$ for this salt were reported by Toyota *et al* [30]. The parameters $b$ and $c$ in the conducting plane as well as the unit-cell volume $V$ were found to decrease with decreasing $T$. Naively, from a qualitative viewpoint one would think that the bandwidth $W$ is proportional to $V^{-1}$. Consequently, $W$ would increase with lowering $T$. A more precise analysis requires one to know how the intradimer and interdimer charge-transfer energies change with $T$, since it is known that the bandwidth is mainly governed by an interdimer transfer energy $t_p$, while the intradimer transfer energy $t_{b1}$ dominates the on-site Coulomb repulsion $U$ [5]. A recent work by Mori *et al* revealed some correlation between these quantities and the structure parameters for several types of ET salt [31]. They noticed that, due to the existence of the polymeric anion chains in ET salts, the structural contraction is anisotropic. They found that the ratio of lattice constants in the conducting plane, $b/c$, correlates well with $t_p/t_{b1}$, or $W/U$, and can be taken as a good measure for the bandwidth. For $\kappa$-$(ET)_2Cu(NCS)_2$, the ratio $b/c$ increases from 0.6431 at room temperature to 0.6561 at liquid helium temperature due to the anisotropic contraction. Accordingly, the bandwidth increases.

In conclusion, our optical study reveals polaron formation in $\kappa$-$(ET)_2Cu(NCS)_2$. At high temperatures, the polarons have small sizes and do not participate in a coherent motion. Accordingly, the conductivity emerges as an activated hopping of self-trapped carriers. At low temperatures, the average size of a polaron increases, and there appears a coherent motion of polarons which gives rise to a metallic behaviour.

## Acknowledgments

We thank S Tajima, T Timusk, and C Homes for valuable discussion and help. This work was supported by research grants from NSFC (No 19974049), Simon Fraser University, and NEDO. The infrared measurement was performed at Simon Fraser University.

## References

[1] Imada M, Fujimori A and Tokura Y 1998 *Rev. Mod. Phys.* **70** 1039
[2] Miyagawa K, Kawamoto A, Nakazawa Y and Kanoda K 1995 *Phys. Rev. Lett.* **75** 1174
[3] Schirber J E, Overmyer D L, Carlson K D, Williams J M, Kini A M, Wang H Hau, Charlier H A, Lore B J, Watkins D M and Yaconi G A 1991 *Phys. Rev.* B **44** 4666
[4] Urayama H, Yamochi H, Saito G, Nozawa K, Sugano T, Kinoshita M, Sato S, Oshima K, Kawamoto A and Tanaka J 1988 *Chem. Lett.* **1988** 55
[5] Kino H and Fukuyama H 1996 *J. Phys. Soc. Japan* **65** 2158
[6] Kawamoto A, Miyagawa K, Nakazawa Y and Kanoda K 1995 *Phys. Rev. Lett.* **74** 3455
[7] Toyota N and Sasaki T 1990 *Solid State Commun.* **74** 361
[8] Cariss C S, Porter L C and Thorn R J 1990 *Solid State Commun.* **74** 1269
[9] Ugawa A, Ojima G, Yakushi K and Kuroda H 1988 *Phys. Rev.* B **38** 5122
[10] Sugano T, Hayashi H, Kinoshita M and Nishikida K 1989 *Phys. Rev.* B **39** 11 387
[11] Kornelsen K, Eldridge J E, Homes C C, Wang H Hau and Williams J M 1989 *Solid State Commun.* **72** 475
[12] Kornelsen K, Eldridge J E, Wang H Hau and William J M 1991 *Phys. Rev.* B **44** 5235

[13] Homes C C, Reedyk M, Crandles D A and Timusk T 1993 *Appl. Opt.* **32** 2976
[14] Emin D 1975 *Adv. Phys.* **24** 305
Emin D 1993 *Phys. Rev.* B **48** 13 691
[15] Yoon S, Liu H L, Schollerer G, Cooper S L, Han P D, Payne D A, Cheong S-W and Fisk Z 1998 *Phys. Rev.* B **58** 2795
[16] Bi Xiang-Xin and Eklund P C 1993 *Phys. Rev. Lett.* **70** 2625
[17] Muhlstroh R and Reik H G 1967 *Phys. Rev.* **162** 703
[18] Bogomolov V N and Mirlin D N 1968 *Phys. Status Solidi* **27** 443
[19] Rice M J and Lipari N O 1977 *Phys. Rev. Lett.* **38** 437
[20] Lipari N O, Rice M J, Duke C B, Bozio R, Girlando A and Pecile C 1977 *Int. J. Quantum Chem. Symp.* **11** 583
[21] Kozlov M E, Pokhodnia K I and Yurchenko A A 1989 *Spectrochim. Acta* **45** 437
[22] Ishiguro T, Yamaji K and Saito G 1998 *Organic Superconductors* 2nd edn (Berlin: Springer)
[23] Visentini G, Masino M, Bellitto C and Girlando A 1998 *Phys. Rev.* B **58** 9460
[24] Shaik S S and Whangbo M H 1983 *Inorg. Chem.* **25** 1201
[25] Munn R W and Siebrand W 1970 *J. Chem. Phys.* **52** 47
Munn R W and Siebrand W 1970 *J. Chem. Phys.* **52** 6391
[26] Holstein T 1959 *Ann. Phys., NY* **8** 325
Holstein T 1959 *Ann. Phys., NY* **8** 343
[27] Kim K H, Gu J Y, Choi H S, Park G W and Noh T W 1996 *Phys. Rev. Lett.* **77** 1877
[28] Lee J D and Min B I 1997 *Phys. Rev.* B **55** 12 454
[29] Kim K H, Jung J H and Noh T W 1998 *Phys. Rev. Lett.* **81** 1517
[30] Toyota N, Watanabe W and Sasaki T 1993 *Synth. Met.* **55–57** 2536
Watanabe Y, Shimizu T, Sasaki T and Toyota N 1997 *Synth. Met.* **86** 1917
[31] Mori T, Mori H and Tanaka S 1999 *Bull. Chem. Soc. Japan* **72** 179
Note that in this paper, the notation for the crystal axes was taken on the basis of κ-(ET)$_2$Cu[N(CS)$_2$]Br. To compare with the notation for κ-(ET)$_2$Cu(NCS)$_2$, one has to make the following substitutions: $a \rightarrow c$; $b \rightarrow a$; and $c \rightarrow b$.